Effect of Sulfur on Characterization of $AgInSe_{1.8}S_{0.2}$ Thin Film and n-$AgInSe_{1.8}S_{0.2}$ / p-Si Solar Cell

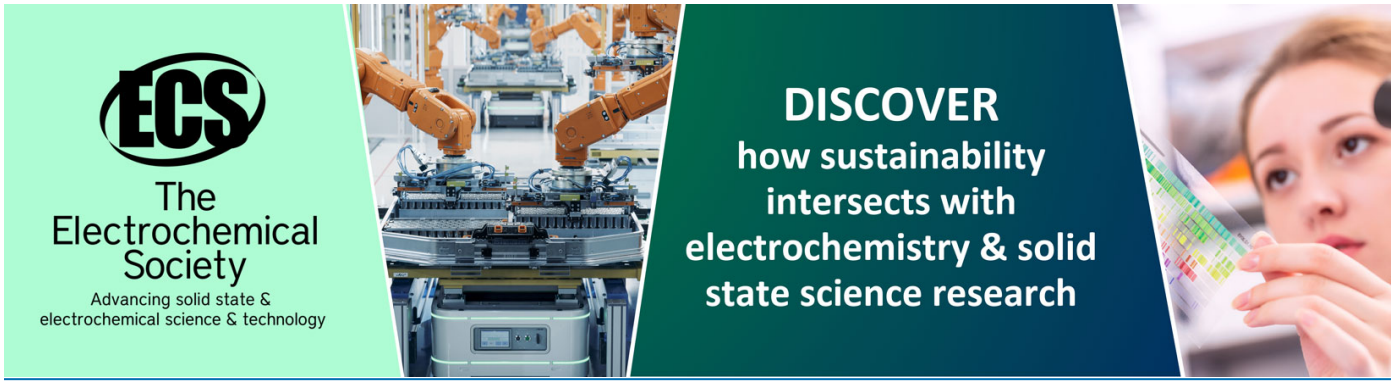

Effect of Sulfur on Characterization of $AgInSe_{1.8}S_{0.2}$ Thin Film and n- $AgInSe_{1.8}S_{0.2}$ / p-Si Solar Cell

Bushra H. Hussein [1,a], Hanan K. Hassun [1], Bushra K.H. Al-Maiyaly [1], Ebtisam M-T. Salman [1], Auday H. Shaban [2], Mohammad Hady Mahdi [1]

[1] Department of physics, College of Education for Pure Science, Ibn Al-Haitham, University of Baghdad, Baghdad, Iraq

[2] Department of Remote sensing & GIS, College of Science, University of Baghdad, Baghdad, Iraq

[a] Corresponding author: boshra.h.h@ihcoedu.uobaghdad.edu.iq

Abstract. Ternary Silver Indium selenide Sulfur $AgInSe_{1.8}S_{0.2}$ in pure form and with a 0.2 ratio of Sulfur were fabricated via thermal evaporation under vacuum 3*10-6 torr on glasses substrates with a thickness of (550) nm. These films were investigated to understand their structural, optical, and Hall Characteristics. X-ray diffraction analysis was employed to examine the impact of varying Sulfur ratios on the structural properties. The results revealed that the $AgInSe_{1.8}S_{0.2}$ thin films in their pure form and with a 0.2 Sulfur ratio, both at room temperature and after annealing at 500 K, exhibited a polycrystalline nature with a tetragonal structure and a predominant orientation along the (112) plane, indicating an enhanced degree of crystallinity. The Atomic Force Microscopy (AFM) was utilized to explore how Sulfur affects roughness of surfaces and sampls Grain Size . Furthermore, optical parameters, such as the optical gap and absorption coefficient, were calculated to assess the influence of Sulfur on the optical properties of the $AgInSe_{1.8}S_{0.2}$ thin films. The UV/Visible measurements indicated a reduction in the energy band gap to 1.78 eV for AgInSe1.8S0.2 at 500 K, making these films potentially suitable for photovoltaic applications. These thin films exhibited donor characteristics, with an increase in electron concentration observed with higher Sulfur content and annealing temperature.

Keywords: $AgInSe_{1.8}S_{0.2}$, Sulfur, thin films, thermal evaporation, Optical parameters.

1. Introduction

Indeed, chalcopyrite thin films such as AgInSe2 exhibit a tetragonal crystalline structure and belong to the family of compounds known as AIBIIIC2VI, where A represents elements like Cu, Ag & B denotes Al, Ga, In, & C represents S, Se, Te. These compounds are analogues to the binary zinc blende II-VI [1]. Indeed, the AgInSe2 (AIS) films possess certain advantages that make them commercially preferable over CIS (Copper Indium Selenide). AgInSe2 has a lower melting point compared to CIS, making it a more viable option for industrial processes. Additionally, the energy gap of Ag compounds films is broader than that of CIS and is near to the optimum range within the solar spectrums. Wider energy gap of AISe is favorable for photovoltaic cells, as it aligns with the desired range for efficient energy conversion. Moreover, AIS exhibits high optical absorption, approximately around 10^5 cm^(-1), which is beneficial for capturing a significant amount of incident light, further establishing its potential as a promising absorber material for photovoltaic applications [2,3]. Several techniques used to fabrication $AgInSe_{1.8}S_{0.2}$, such as thermal evaporation with the ion irradiation [4] spray pyrolysis technique [5,6]. hot-press method [7]. Sequentially deposited nano-films under vacuum [8] electrodeposition process with heat treatment at 593 K [9] thermal evaporation with vacuum annealing [10] Deposition of chemical bath [11] DC magnetron sputtering [12], incorporation reactive evaporation [13] sol–gel spin-coating technique [14] such as co-evaporation [15] hybrid sputtering/evaporation process [16]. pulsed electrodeposition technique [17]. transition type of semiconductors is direct gap [15] All crystal structures of AgInSe2 (AIS) are tetragonal structures known as chalcopyrites with specific lattice constants. The lattice constants for this structure are a = b = 6.102 Å and c = 11.69 Å. These values determine the dimensions of the unit cell within the tetragonal crystal lattice of AgInSe2.

[6]. Absolutely, the type of conductivity exhibited by materials like AgInSe2 (AIS) can vary and can be either n-type or p-type. This classification depends on the dominant carrier within the material, which can be either electrons (n-type conductivity[18]) or holes (p-type conductivity [9]). The behavior is determined by the presence of specific impurities or doping elements and their impact on the semiconductor material [19]. Certainly, various studies have explored the impact of different material doping on AgInSe2 thin films. For instance, one such study investigated the effects of the boron adding on AISe by employing ions implantation at different annealing temperatures ranging from 473 to 673 K [2] The influence of germanium(Ge) doping [18]. The effect of Tin (Sn) on electrical conductivity enhancements and the band gap [13]. The effects of Zinc doping have been observed to cause specific changes in its characteristics. When Zn substitutes for Ag within AgInSe2, it forms active donor defects. This causes a shift of the Fermi level towards the conduction band, leading to an increase in the carrier concentration [20,21]. The effects of Copper on Ag0.8Cu0.2InSe2 Fabrication and study the influence of vacuum annealing (473,573) K on structure and optical properties [10] The efficiency 3.07% of silver indium selenide with Zinc-diffused [22] the highest efficiency (η = 1.68%) of p-ZnTe/n-AgCuInSe2/p-Si [23] In this study the role of Sulfur S with ratio 0.2 in AIS occupies the anion (Se) and the relatively electronegativity of S (2.58) compared with Ag (1.93), In (1.78), Se (2.55), the selenide and Sulfur are part of the elements of the third period and group VI from Periodic Table [24].
The goal of this research is to investigate the influence of sulfur (S) on the optical, structural properties, and Hall Effect of AgInSe2 (AIS) thin films. This research aims to explore and establish the relationship between these parameters, seeking to understand how the addition of sulfur impacts the structural characteristics, optical behavior, and the electrical properties (such as the Hall Effect) of AIS films. The interconnection and correlations between these aspects are central to uncovering the comprehensive impact of sulfur on the overall properties and behavior of AgInSe2 thin films.

2. Experimental

The $AgInSe_{1.8}S_{0.2}$ thin film was prepared by first synthesizing an alloy of Silver Indium Selenide Sulfur from highly pure (99.999%) elements in stoichiometric proportions (1:1:1.8:0.2). These elements were combined in an evacuated quartz tube at a pressure of 5×10^{-4} mbar and heated to 950 K for seven hours, and then allowed to cool to room temperature. The thin films of AgInSe1.8S0.2 were subsequently deposited using the thermal evaporation method on glass substrates with a thickness of 550 nm, employing a vacuum system of 3×10-6 torr.
X-ray diffraction was utilized to analyze the structure composition of those film by assessing 2Θ within the range of 20° to 80° by a 0.05° interval. The formula of Scherer's was applied to compute the size of crystalline for the samples [25- 27]. Atomic force microscopy revealed that the morphology of surface, roughness & Grain Size was influenced by the 0.2 ratio of S content and the annealing temperature.
The thickness of AIS and $AgInSe_{1.8}S_{0.2}$ samples was determined using the optical interferometer method. Additionally, the optical properties were assessed by noting transmission and absorption spectrums within the 400 to 1000 nm range, calculating absorption coefficients (α) and the energy gap (Egopt) using Lambert's Law and Tauc equation, respectively [28-31]. Optical constants were also considered [32,33].
The Hall Effect was examined using Van der Pauw's method (Ecopia-HMS -3000) to ascertain the nature of the thin films of AIS and $AgInSe_{1.8}S_{0.2}$.

3. Results and discussions

Figure (1) illustrates the X-ray diffraction (XRD) patterns for both the pure AgInSe2 and $AgInSe_{1.8}S_{0.2}$ films at room temperature (RT) and after annealing at 500 K, with a deposition thickness of (550) nm on a glass substrate. The XRD pattern for AgInSe2 films displays a polycrystalline nature, showing a tetragonal structure with two main peaks: one around $2\theta \approx 25.726°$, exhibiting a preferred orientation of (112)[1,5], and another peak at $2\theta \approx 42.97°$.
Table (1) in our study indicates a strong correspondence with the standard value from the ICDD 00-038-0952 card, suggesting a highly matched degree of crystallinity. The degree of crystallinity increased

notably with a Sulfur ratio of 0.2 and after annealing at 500 K. The main intensity of the (112) peak increased upon the addition of Sulfur, shifting approximately 2° to a lower 2θ angle compared to the AgInSe2 films. This shift can be attributed to the smaller atomic "radius" of S (0.43 Å) in comparison to Se (0.56 Å). This increase in intensity signifies the inclusion of Sulfur atoms in the Se vacancies, leading to enhanced crystallinity.

The crystal structure and orientation of the thin films remained consistent even after the addition of 0.2 Sulfur content. The relationship between the Full Width at Half Maximum (FWHM) of the primary peak and the Sulfur content (0.2) is detailed in the same table, revealing a decrease in FWHM with added Sulfur content, subsequently resulting in increased crystallite size.

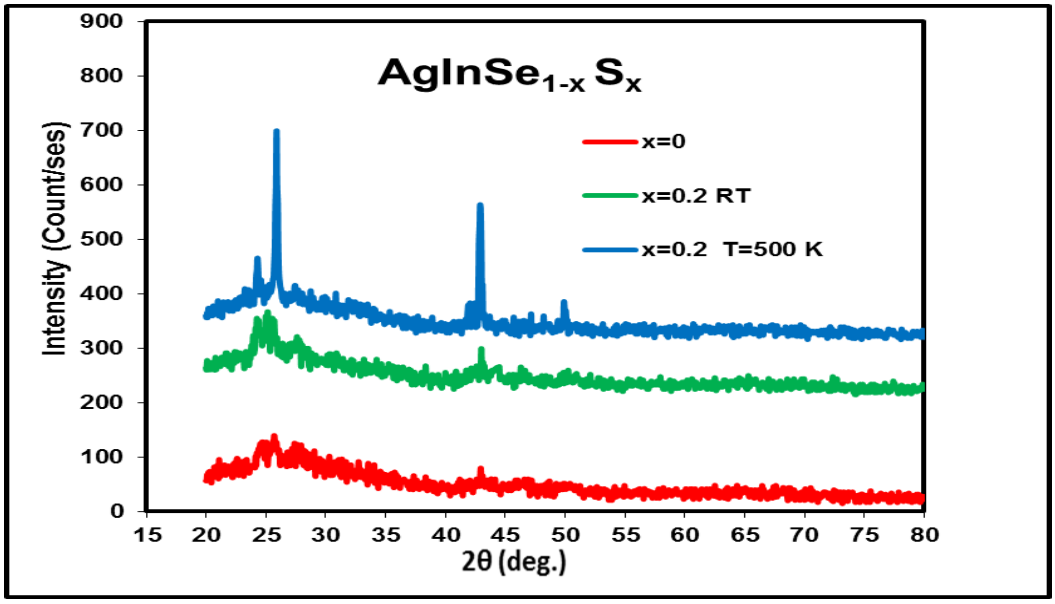

Figure 1. Pattern of XRD for $AgInSe_{1-x}S_x$ (x=0, 0.2 (RT), 0.2(T=500 K)) film.

Table 1. XRD data AgInSe1-x Sx (x=0, 0.2 (RT), 0.2(T=500 K)) film.

Thin Films $AgInSe_{1-x}S_x$	**d(Std.) (Å)**	**d(Exp.) (Å)**	**2θ (Std.) (Deg.)**	**2θ (Exp.) (Deg.)**	**hkl**	**FWHM (deg.)**	**C.S (nm)**
x=0	3.46	3.4651	25.726	25.7	112	1.250	6.809
	2.103	2.1012	42.97	42.95	204		
x=0.2 RT	3.46	3.4776	25.726	25.5	112	0.600	14.18
	2.103	2.1017	42.97	43	204		
x=0.2	3.46	3.4373	25.726	25.38	112	0.347	24.513
T=500 K	2.103	2.1069	42.97	42.9	204		

In Figures (2), the AFM topographical images of the $AgInSe_{1-x}S_x$ (x=0, 0.2 (RT), 0.2(T=500 K)) thin films are presented. Atomic Force Microscopy (AFM) has provided valuable insight into the microsurfaces, offering previously inaccessible details. The analysis from AFM work revealed that the surfaces of all films showcase numerous small-sized grains with a uniform distribution, affirming the polycrystalline structure identified from the XRD analysis.

Table (2) demonstrates that with the addition of 0.2 Sulfur content and through annealing, the average grain size of the films increases. This enlargement aligns with the anticipated increase in the crystallite size of the thin films, consistent with findings by Sobhi S.N [3].

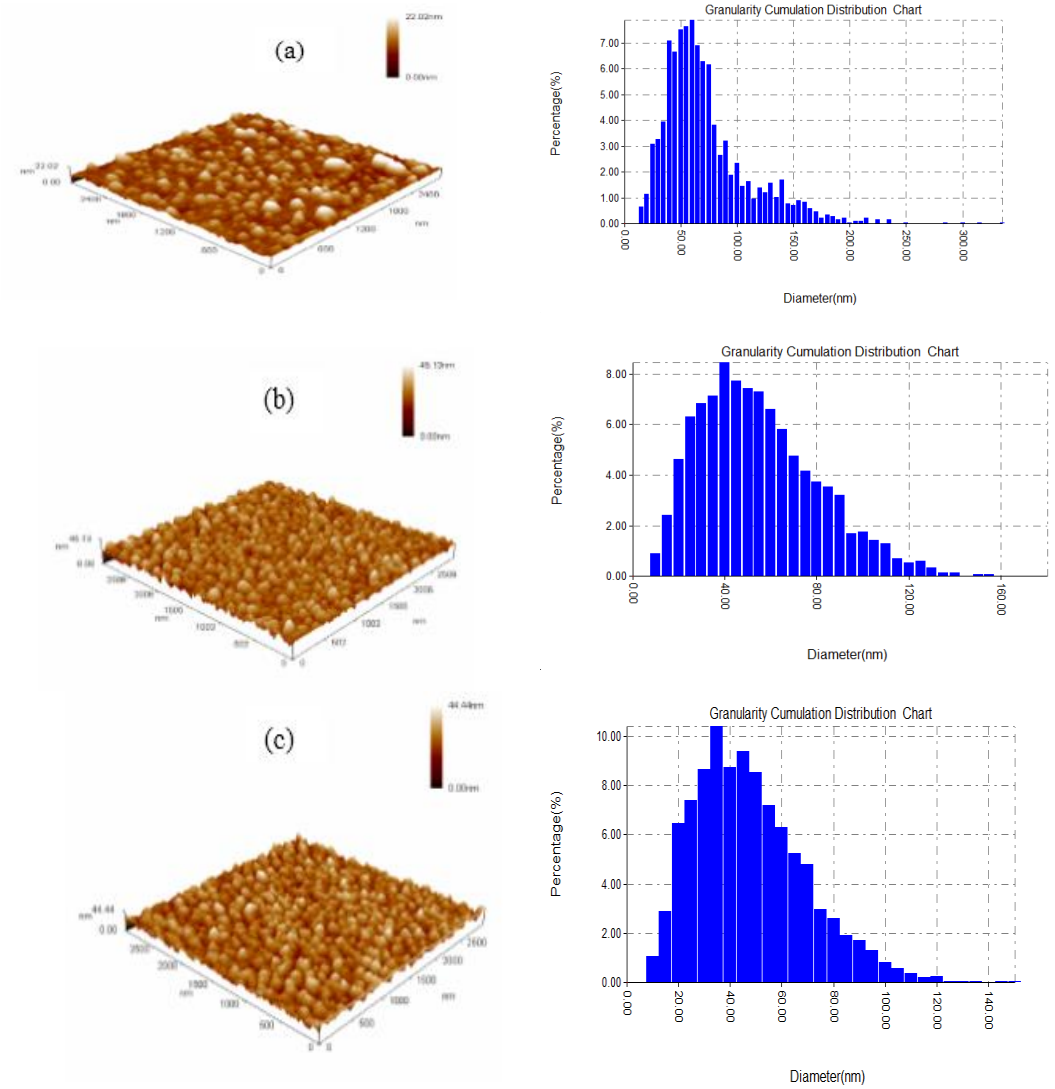

Figure 2. AFM micrographs of $AgInSe_{1-x}S_x$ ((a) x=0, (b) 0.2 (RT), (c) 0.2(T=500 K))

Table 2. AFM analysis data for $AgInSe_{1-x}S_x$ ((a) x=0, (b) 0.2 (RT), (c) 0.2(T=500 K))

Thin Films $AgInSe_{1-x}S_x$	Surfaces roughness (nm)	Root mean Sq. (nm)	Grain Size (nm)
x=0	1.25	2.51	45.53
x=0.2 RT	4.22	5.2	51.56
x=0.2 T=500 K	4.35	5.38	52.61

Figure (3) and Table (3) showcase the optical properties and the impact of a 0.2 Sulfur's annealing and ratio at 500K on the absorbance spectra and transmittance of $AgInSe_{1-x}S_x$ film. Notably, the absorbance of the thin film is directly proportional with the increases of the 0.2 Sulfur ratio and the 500K annealing temperature, likely due to enhanced crystallinity and larger Grain Size.

Using the Tauc Equation, the value and type of the gap of optical energy for $AgInSe_{1-x}S_x$ thin films, particularly after annealing at 500K, have been determined, indicating allowed direct transitions within these films. This finding aligns with R. Panda et al.'s work [4]. The absorption coefficients (α) of approximately 10^4 were calculated from the absorbance spectra of these films.
Figure (4) illustrates a noticeable decrease in the energy gap, potentially linked with advancement in the films' size of crystallite. The energy gap calculated in values which are detailed in the Table (3). Furthermore, the the refractive index (n) values, the coefficient extinction (k), and the imaginary and real parts of the constant for the dielectric (εr, εi) for the $AgInSe_{1-x}S_x$ thin film are depicted in Figure (5) and called out in Table (3). The index of refractive (n), an important optical material parameter, exhibits a decrease with the addition of Sulfur and an increase in annealing temperature at a wavelength of 400nm. This decrease in n is attributed to the corresponding reduction in reflection and an increase in carrier concentrations in the $AgInSe_{1-x}S_x$ thin film, aligning with findings by Suresh Pal et al. [34,35]. The coefficient of extinction (k) shows similarities in behavior to the coefficient of absorption, increasing in response to the addition of Sulfur, as detailed in Table (3). The complex dielectric constant describes the fundamental electron excitation spectrum of the films. Both the real (εr) and imaginary (εi) parts of the dielectric constant at λ=400nm decrease, following similar trends as n and k. The impact of the 0.2 Sulfur ratio and annealing on the value of εi was smaller than of the pure thin films, indicating a reduced loss in the dielectric constant.

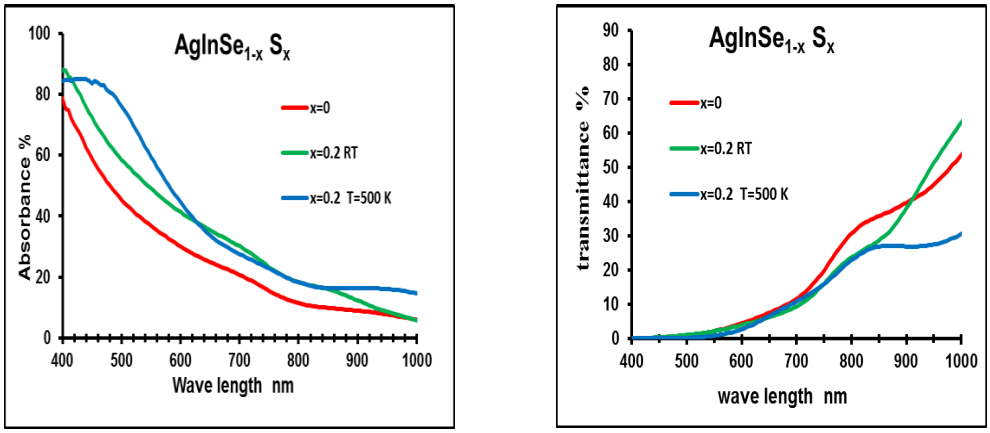

Figure 3. Absorption and Transmittance with the wave length for $AgInSe_{1-x}S_x$ (x=0, 0.2 (RT), 0.2(T=500 K))

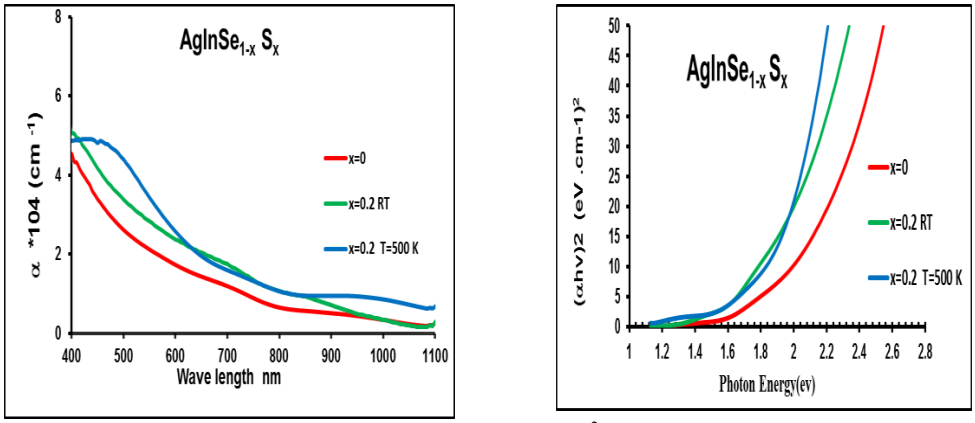

Figure 4. The Wavelength vs. α and hυ plot vs. $(\alpha h\upsilon)^2$ of as prepared **$AgInSe_{1-x}S_x$ (x=0, 0.2 (RT), 0.2(T=500 K))**

Table 3. The parameters of optical (k, n, E_g^{opt}, α, εi and εr)for $AgInSe_{1-x}S_x$ (x=0, 0.2 (RT), 0.2(T=500 K)) thin films where λ=400nm

$AgInSe_{1-x}S_x$	E_g^{opt} (eV)	$\alpha\times10^4$ cm^{-1}	n	k	εr	εi
x=0	**1.95**	4.6	1.85	0.14	3.4	0.53
x=0.2 (RT)	**1.8**	3.37	1.5	0.16	2.3	0.49
x=0.2(T=500 K)	**1.78**	4.39	1.65	0.15	2.7	0.51

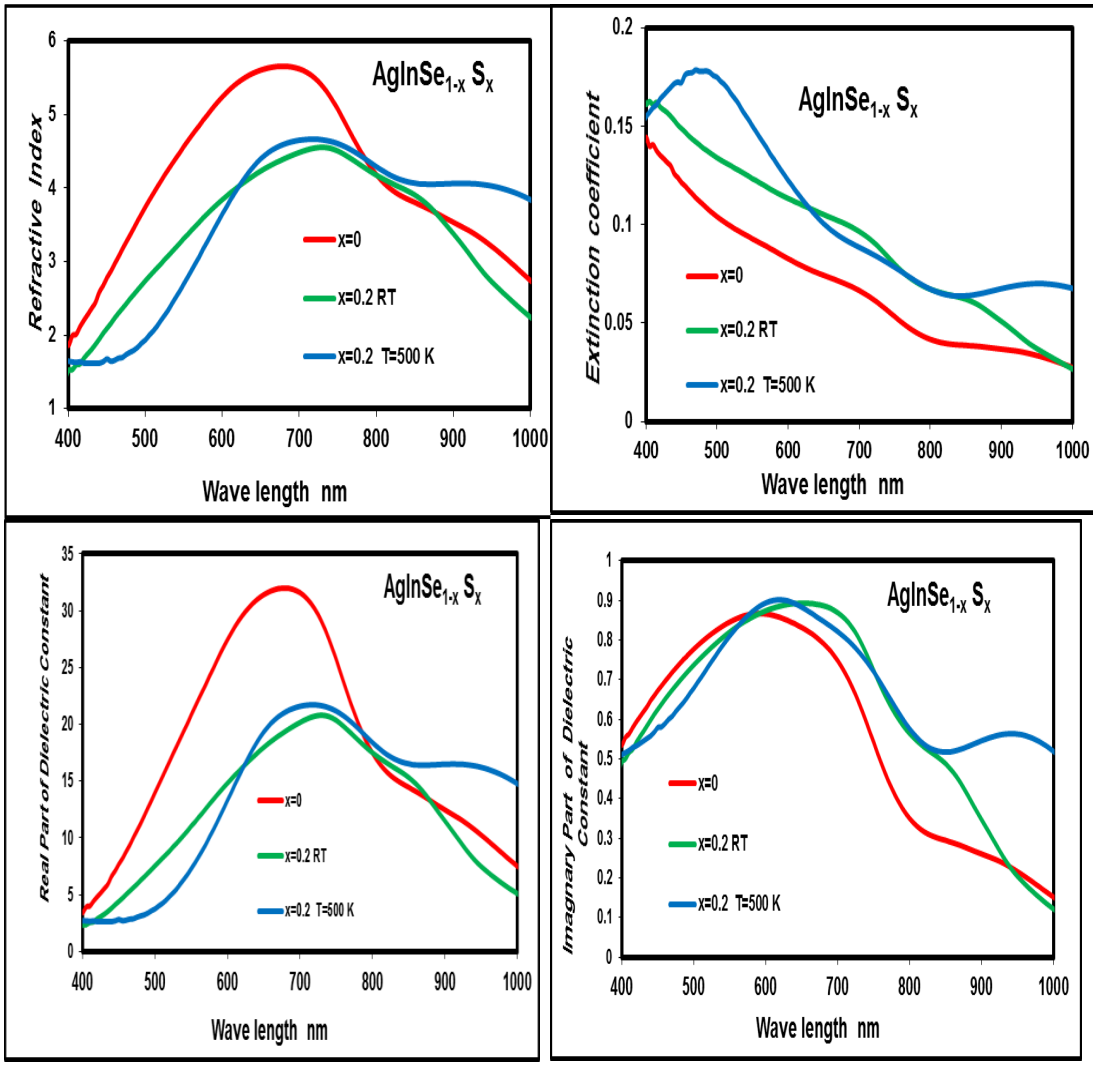

Figure 5. Variation of refractive index n, Extinction coefficient k, real and imaginary part of dielectric constants for $AgInSe_{1-x}S_x$ (x=0, 0.2 (RT), 0.2(T=500 K))

From Hall effect measurements, the type and concentration of charge carriers, along with the Hall mobility, were determined for the $AgInSe_{1-x}S_x$ thin films at a Sulfur ratio of 0.2 and annealing at 500 K. The calculated values are detailed in Table (4).

Observing Table (4), it's evident that the Hall coefficient for all the investigated $AgInSe_{1-x}S_x$ thin films is negative. This indicates that all the prepared samples exhibit n-type conductivity, implying that the conduction is primarily dominated by electrons. This behavior is attributed to the donor centers formed during the deposition process, aligning with findings from previous investigations [18].
Additionally, it's notable that the carrier concentration increases as the annealing temperature rises. This increase in carrier concentration is due to the enlargement of the film's grain size, subsequently reducing the density of grain boundaries and minimizing the electron trapping probability. However, this rise in carrier concentration comes with a decrease in mobility as the annealing temperature increases. The larger grain size leads to a decrease in the number of collisions between carriers, ultimately resulting in a decline in their mobility with increasing annealing temperature.

Table 4. Hall effect parameters for $AgInSe_{1-x}S_x$ (x=0, 0.2 (RT), 0.2(T=500 K))

$AgInSe_{1-x}S_x$	R_H (cm^3/C)	N_D (cm-3)	μ_H ($cm^2/V.s$)	ρ(Ω.cm)
x=0	-25	$2.5*10^{17}$	5	5
x=0.2 (RT)	-16.5	$3.8*10^{17}$	213	0.077
x=0.2(T=500 K)	-11	$5.7*10^{17}$	208	0.053

The variations in photovoltaic parameters for $AgInSe_{1-x}S_x$ including the impact of a Sulfur ratio of 0.2 and annealing at 500K, derived from current-voltage measurements, are outlined in Table 5. Figure 4 illustrates the current-voltage (I-V) curves for three devices constructed from the same $AgInSe_{1-x}S_x$ /Si heterojunction with different annealing temperatures under illumination at incident light power levels of 10^2mW/cm2.
The efficiency of the $AgInSe_{1-x}S_x$ devices increases, notably due to the rise in Jsc values, which stem from the reduction in the energy gap value observed in the study of optical properties. Simultaneously, there is an increase in the values of the open-circuit voltages (VOC). This increase in VOC is associated with the elevated carrier concentration, the enhanced surface roughness, and the absorption coefficient [3].

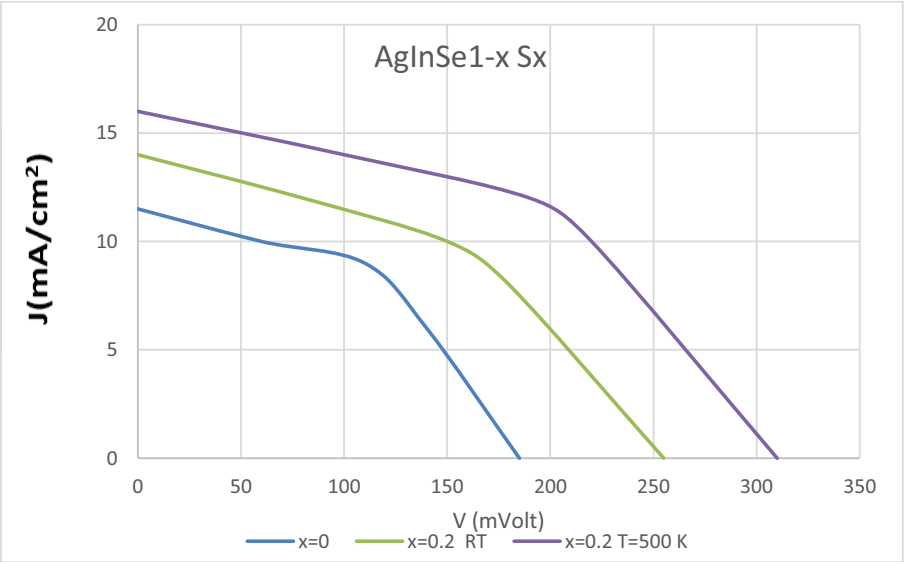

Figure 6. I-V Characteristic under illumination for $AgInSe_{1-x}S_x$ /Si solar cell (x=0, 0.2 (RT), 0.2(T=500 K))

Table 5. Parameters of Light I-V solar cell for $AgInSe_{1-x}S_x$ /Si solar cell (x=0, 0.2 (RT), 0.2(T=500 K)

Thickness(550 nm) $AgInSe_{1-x}S_x$ /Si	**x=0 RT**	**x=0.2 (RT)**	**x=0.2 (T=500 K)**
Voc (mVolt)	185	225	310
J_{sc} (mA/cm^2)	11.5	14	16
Vmax (mVolt)	110	150	190
Jmax (mA/cm2)	9	10	12
Fill factor	0.46	0.47	0.456
Efficiency	0.99	1.5	2.28

4. Conclusions

The $AgInSe_{1-x}S_x$ /Si solar cell, synthesized as an undoped chalcopyrite with 0.2 of Sulfur (S) and annealed at 500 K, was successfully fabricated using the thermal evaporation method on glass substrates. Our findings, gathered through various analyses, indicate significant outcomes: The X-ray diffraction (XRD) results displayed a polycrystalline tetragonal structure with a (112) orientation for the AgInSe2 thin film. The grain size was observed to increase with the addition of 0.2 of Sulfur, indicating an improvement in the grain structure. Optical studies revealed a reduced band gap when Sulfur was added, compared to the undoped AgInSe2 chalcopyrite. This addition of Sulfur also led to an increase in absorption coefficients, enhancing the film's optical properties. The Hall effect analysis demonstrated that all the thin films exhibit n-type behavior, further highlighting the favorable impact of 0.2 of Sulfur in making these films suitable for photovoltaic applications. The efficiency of the solar cell increased notably after annealing, reaching maximum values of 0.99 and 2.25 at an annealing temperature of 500 K. This improvement in efficiency underscores the potential for these films in practical photovoltaic applications.

References

[1]R. K. Bedi, D. Pathak, Deepak and D. Kaur, 2008 *Z. Kristallogr. Suppl.,* **27** 177-183.
[2] T C¸olako˘glu,, M Parlak, M Kulakci and R Turan*, J. Phys. D: Appl. Phys*., 2008, **41**.
[3] Sobhi S.N., Hussein B.H., Effect of annealing on thin film AgInSe2 solar cell, Journal of Ovonic Research, 2022, 18(4), 519 – 526.
[4] R. Panda, S. A. Khan, U. P. Singh, R. Naik and N. C. Mishra, *RSC Adv.*, 2021, **11**, 26218–26227.
[5] F. A. MAHMOUD and M. H. SAYED 2011 *Chalcogenide Letters* **8** 595 – 600.
[6] Qian Cheng, Xihong Peng, and Candace K. Chan 2013 *ChemSusChem,***6** 102 – 109.
[7] S Kenji Yoshino, Aya Kinoshita, Yasuhiro Shirahata, Minoru Oshima, Keita Nomoto, Tsuyoshi Yoshitake, Shunji Ozaki, Tetsuo Ikari, *Journal of Physics: Conference Series*, 2008, **100**.
[8] H. Essaidi, A. Gantassi, S. Touihri, J. Ouerfelli, Tuning the structural, optical and electrical properties of AgInSe2 thin films prepared by sequentially deposited silver and indium nano-films under vacuum, Optik, 2019, **182**, 866-875.
[9] Mounir Ait Aouaj, Raquel Diaz, Fouzia Cherkaoui El Moursli, *International Journal of Materials Science and Applications*, 2015, **4**, 35–38.
[10] Athab, R.H., Hussein, B.H., Preparation and study effect of vacuum annealing on structure and optical properties of AgCuInSe2 thin film, Digest Journal of Nanomaterials and Biostructures, 2022, **17**(4), 1173 – 1180.
[11] Ching-Chen Wu, Kong-Wei Cheng, Wen-Sheng Chang and Tai-Chou Lee, *Journal of the Taiwan Institute of Chemical Engineers*, 2009, **40**,180-187.
[12] R. Panda, R. Naik, U.P. Singh, N.C. Mishra, *International Conference on Materials Science & Technology*, 2016, Oral / Poster.
[13] Rajani Jacob, Gunadhor S. Okram, Johns Naduvath, Sudhanshu Mallick, and Rachel Reena

Philip, *The Journal of Physical Chemistry C*, 2015, **119**, pp. 5727−5733.
[14] F. A. Al-Agel and Waleed E. Mahmoud, *Journal of Applied Crystallography*, 2012, **45**, 921-925.
[15] C. A. Arredondo, F. Mesa1, and G. Gordillo1, *IEEE*, 2010, **978**, 002433–002438.
[16] S. A. Little, V. Ranjan, R. W. Collins, and S. Marsillac, 2012 *Appl. Phys. Lett.,* **687**.
[17] H. R. Kulkarni 2016 Journal of Management Science & Technology 7, 190–197.
[18] Yoshinori Ema, Hiroshi Kato andTakahiro Takahashi, *Japanese Journal of Applied Physics* 2002, **44** (3A), 1527-1531.
[19] Jeoung Ju Lee, Jong Duk Lee, Byeong Yeol Ahn, Hyeon Soo Kim and Kun Ho Kim, *Journal of the Korean Physical Society*, 2007, **50**, 1099–1103.
[20] Li Wang, Pengzhan Ying, Yuan Deng, Hong Zhou, Zhengliang Du and Jiaolin Cui, *The Royal Society of Chemistry,* 2014, **4**, 3897–33904.
[21] AnaamW.Watan, Suad H.Aleabi, Ridha H. Risan, Kareem A. Jasim, Auday H. Shaban, Preparation and Physical Properties of Doped CdBa2-x SrxCa2Cu3O8+δCompound, Energy Procedia, Vol.119c, pp:466-472, 2017.
[22] Ganga Halder and Sayan Bhattachary, Thin Solid Films, 2005, 480–481, 452–456.
[23] R. H. Athab, B. H. Hussein, Chalcogenide Letters 2023, Vol. 20, No. 2, p. 91 - 100.
[24] R. D. Shannon, Acta Crystallogr A., 1976, 32 (5), 751–767.
[25] Rana H. Athab, Bushra H. Hussein, and Sameer A. Makki, AIP Conference Proceedings, 2019 2123, 020030-1- 020030-9.
[26] B. H. Hussein, H. K. Hassun, B. K.H. Al-Maiyaly, S. H. Aleabi, Journal of Ovonic Research, 2022, 18 (1), 37-41.
[27] Aqeel N. Abdulateef, Ahlam Alsudani, Riyadh Kamil Chillab, Kareem A. Jasim, Auday H. Shaban, Calculating the Mechanisms of Electrical Conductivity and Energy Density of States for Se85Te10Sn5-xInx Glasses Materials, Journal of Green Engineering (JGE), Volume-10, Issue-9, September 2020, pp: 5487–5503, 2022.
[28] R.H. Athab and B.H. Hussein, "Growth and Characterization of Vacuum Annealing AgCuInSe2 Thin Film", Ibn al-Haitham J. Pure Appl. Sci., 35(4) (2022) 45-54.
[29] S.Sze and K.Ng., Physics of Semiconductor Devices, 3rd edition, John Wiley and Sons, 2007; https://doi.org/10.1002/0470068329
[30] Riyadh Kamil Chillab, Sarab Saadi Jahil, Kassim Mahdi Wadi, Kareem A. Jasim, Auday H. Shaban, Fabrication of Ge30Te 70-xSbx Glasses Alloys and Studying the Effect of Partial Substitution on D.C Electrical Energy Parameters, Key Engineering Materials, Vol. 900, pp 163-171, 2021.
[31] Almaiyaly, Bushrak H., Hussein, Bushra H., Auday H. Shaban, Fabrication and characterization study of ZnTe/n-Si heterojunction solar cell application, Journal of Physics: Conference Series, 2018, Volume 1003, Issue 1
[32] B. K. H. Al-Maiyaly, B. H. Hussein, H. K. Hassun, Journal of Ovonic Research, 16 (5), 267 - 271 (2021).
[33] Bushra H. Hussein, Hanan K. Hassun, NeuroQuantology, 18(5) (2020) 77-82; https://doi.org/10.14704/nq.2020.18.5.NQ20171
[34] Suresh Pal, Rajendra Kumar Tiwari, Dinesh Chandra Gupta and Ajay Singh Verma, Journal of Materials Physics and Chemistry, 2014, 2 (2) ,20-27.
[35] Jasim, K.A., Mohammed, L.A., The partial substitution of copper with nickel oxide on the Structural and electrical properties of HgBa2 Ca2 Cu3xNix O8+δ superconducting compound, Journal of Physics: Conference Series, 2018, 1003(1), 012071